ELSEVIER

Chemical Engineering Journal 121 (2006) 125–134

Chemical Engineering Journal

www.elsevier.com/locate/cej

Development and modeling of a rotating disc photocatalytic reactor for wastewater treatment

Lianfeng Zhang [a], William A. Anderson [a,*], Zisheng (Jason) Zhang [b]

[a] *Department of Chemical Engineering, University of Waterloo, 200 University Avenue West, Waterloo, Ontario, Canada N2L 3G1*
[b] *Department of Chemical Engineering, University of Ottawa, Ottawa, Ontario, Canada K1N 6N5*

Received 25 July 2005; received in revised form 24 March 2006; accepted 29 March 2006

Abstract

A photon-effective rotating disc photocatalytic reactor configuration was proposed and compared to a similar rotating drum reactor. The photocatalytic degradation of a model non-volatile aromatic compound, 4-chlorophenol, was investigated as a function of rotation speed, angle of disc, and radiation intensity. The irradiance distribution on the surface of the disc/drum was analyzed by a diffuse emission model, which was verified by experimental measurement. The profiles of the predicted local-area-specific rate of energy absorption (LASREA) indicated its sensitivity to the geometrical dimensions. A new kinetic model was proposed including the effects of water film thickness and irradiance. Based on the model and irradiance distribution, a rigorous kinetic analysis was conducted in accordance with mass balance and mass transfer. The experimental data were compared with the mathematical prediction, showing good agreement. With respect to scale-up parameters, the results suggested that the surface velocity, $\phi\omega/2$ (ϕ: diameter of the disc, ω: rotation speed) is an important factor which determines the thickness of water film, while diameter and angle of the disc determine the irradiance distribution. The incident photon flow rate has no relation to the angle of the disc, but a small angle will provide a larger illuminated area and capture more reflected photons. Comparatively, the larger illuminated area is much more important than capture of reflected photons for improvement of the photonic efficiency. In the rotating disc reactor, the photon number increased 11.2% due to capture of reflections, and the maximum initial photonic efficiency reached 0.0251 mol-4-CP/einstein, while in the drum reactor it was 0.0145 mol-4-CP/einstein.

Keywords: Photocatalyst; Titanium dioxide; Radiation distribution; Reactor; Modeling

1. Introduction

Since the photocatalytic function of the TiO_2 semiconductor was reported in *Nature* [1], photocatalytic technology has attracted much attention for environmental purification, especially, in the latest two decades. Due to its stability and non-toxicity, the TiO_2 photocatalyst is a promising alternative technology for the treatment of wastewater with low concentration, toxic organic pollutants.

When a UV photon is absorbed by the TiO_2 semiconductor, the electrons in the valence band may be excited to jump to the conduction band, leaving positive holes in the valence band. These photogenerated electrons and positive holes will initiate a series of redox reactions to produce hydroxyl and peroxyl radicals, which are powerful oxidants. The photocatalytic purification of water applies such strong oxidant species to oxidize the organic pollutants. The advantage of such oxidation processes is that they can not only decompose but also mineralize the organic pollutants. Since the hydroxyl and peroxyl radicals have very short lifetime [2], the photocatalytic reaction occurs on the surface of the photocatalyst and/or in very close proximity. Thus photocatalytic reactors with thin water films have been suggested [3–7]. In these reactors, there is only a thin water film between the light source and photocatalyst, so the photon loss through absorption in the liquid phase is diminished. It has been revealed that a low UV dose has a higher photonic efficiency [8]. When the light source is fixed, sacrificing a little of the UV intensity to get a larger illuminated area per unit volume is an effective consideration for fabrication of the photocatalytic reactor.

Therefore, a powerful and energy efficient photocatalytic reactor should ideally possess: (1) a large catalyst surface area per unit reactor volume, (2) the capability to continuously or periodically deliver artificial and/or solar radiation to a large

* Corresponding author. Tel.: +1 519 888 4567x5011; fax: +1 519 746 4979.
E-mail address: wanderson@uwaterloo.ca (W.A. Anderson).

1385-8947/$ – see front matter © 2006 Elsevier B.V. All rights reserved.
doi:10.1016/j.cej.2006.05.011

Nomenclature

a	coefficient ($\mu m^{-0.5}$ h)
b	coefficient (μm)
c	speed of light (=3×10^8 m s^{-1})
$C(t)$	4-CP concentration at t time (g m^{-3})
C_0	initial 4-CP concentration (g m^{-3})
C_{O_2}	the concentration dissolved in water (g m^{-3})
$Cr(t)$	mass flow rate into water tank from drum/disc at t time (g h^{-1})
d_1	distance between illuminating point of lamp and illuminated point of upper wing (m)
d_2	distance between reflection-illuminating point of upper wing and illuminated point of lower wing (m)
D	diffusion coefficient of oxygen in water (2.01×10^{-5} cm^2 s^{-1} at 20° C)
F	specific irradiance in the direction of $\psi_1 = \psi_2 = 0°$ (W m^{-2})
h	Planck's constant (=6.63×10^{-34} J s)
I	incident irradiance (W m^{-1})
k	model parameter (m h^{-1})
K	model parameter (m^3 g^{-1})
L	the length of rotating drum (m)
$M_{4\text{-CP}}$	the molar mass of 4-CP (g mol^{-1})
n	model parameter
N_A	Avogadro's number (=6.023×10^{23})
N_{O_2}	the diffusive flux of oxygen in the water film (g m^{-2} s^{-1})
q_0	reference value of LASREA (=10^{-5} einstein m^{-2} s^{-1})
$q(\theta, z)$	LASREA at (θ, z) (einstein m^{-2} s^{-1})
Q	water flow rate onto drum from water tank (m^3 h^{-1})
r	distance between illuminating and illuminated points (m)
r_b	the radius of large side of disc (m)
r_s	the radius of small side of disc (m)
R	the coordinate in the radial direction of rotation for disc/drum
S	illuminated area (m^2)
t	experimental time (h)
V	volume of solution in the tank (m^3)
w_p	incident irradiance at illuminated point (W m^{-2})
w_λ	spectral irradiance, i.e., irradiance from the component of light with wavelength λ (W m^{-2})
W	irradiance of light source (W m^{-2})
z/B	z value in coordinate/half of the distance between two discs (m/m)

Greek symbols

α	half of disc angle (=30°)
δ	thickness of water film (m)
θ	angle coordinate value in polar coordinates (°)
θ_{end}	angle coordinate value of the point (line) that drum/disc contacts water surface when moving into water (°)
λ	light wavelength (nm)
φ	incident photon flow rate (einstein h^{-1})
ϕ	diameter of drum/disc (m)
Φ	photonic efficiency (mol $einstein^{-1}$, based on incident photon flow rate)
ψ_1	angle between vertical direction of lamp plane and illumination direction (°)
ψ_2	angle between vertical direction of illuminated plane and illumination direction (°)
ψ_3	angle between vertical direction of lower wing and reflection-illuminating direction (°)
ψ_4	angle between vertical direction of reflection-illuminated plane (upper wing) and illumination direction (°)
ω	rotation speed (rph)

catalyst surface, (3) sufficient mass transfer capacity between the liquid bulk and the reaction sites, and (4) ability for the catalyst to recapture photons reflected from the catalyst surface.

Accordingly, in this work a rotating disc reactor configuration was proposed. In previous studies, it was demonstrated that: (1) the rotation [9] can create a thin water film and effectively make use of photons, (2) a corrugated surface [10] can increase the illuminated area and recapture reflected photons. In the present work, we combined these two advantages. The radiation field and reaction kinetics were analyzed experimentally and mathematically, and important factors for scale-up are discussed.

2. Experimental

2.1. Materials and method

The configuration of the reactor is shown in Fig. 1(a). The reactor consists of a rotating cylinder (ϕ 77 mm × 204 mm) with multiple teeth, of which the depth is 11.2 mm, to form discs on which Degussa P25 TiO_2 catalyst is immobilized. The immobilization method is reported elsewhere [9]. For comparison purposes, a rotating drum reactor was also constructed with the same dimensions, consisting of a smooth cylinder onto which the TiO_2 was likewise immobilized (not shown). The disc/cylinder was partially immersed in the water tank that contained 160 ml for all experiments. Due to the geometrical differences, the distance between water surface and the centre of the disc/cylinder was 15 mm (60° teeth), and 5 mm (without teeth), respectively. The disc/cylinder was illuminated from above. The disc rotated under illumination provided with three 40 W UV lamp(s) (Philips, TLK 40 W/10R R-UVA). The three lamps were mounted beside each other to form a larger illuminator (515 mm × 114 mm), which was treated as a lamp plane parallel to the water surface. The distance between the lamp plane and the top of disc/cylinder was 5 mm. The control of radiation intensity was realized by

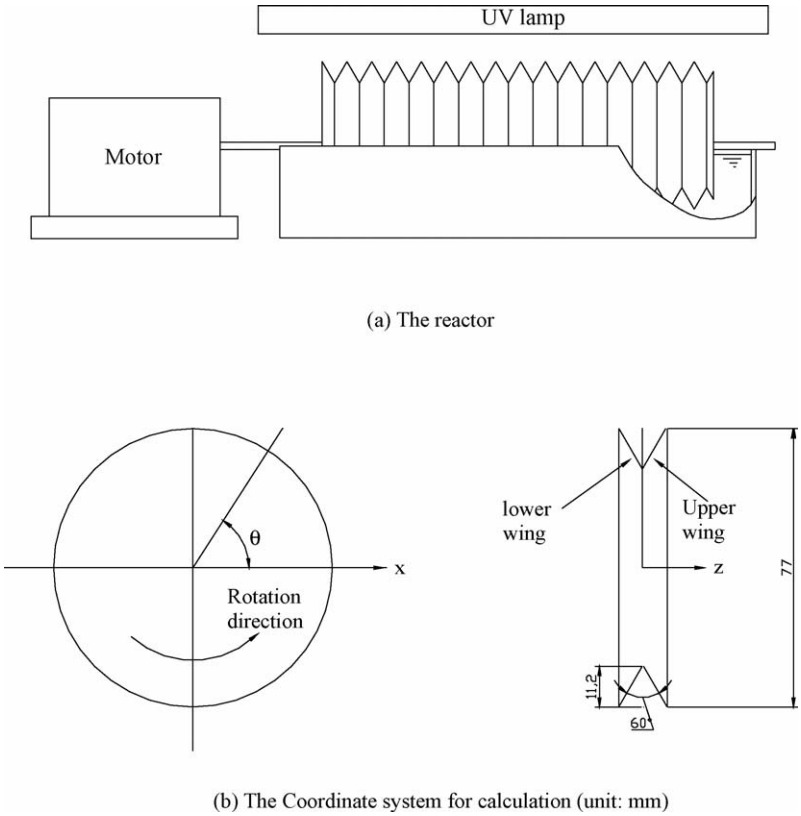

Fig. 1. (a) Photocatalyst coated rotating disc reactor; (b) coordinate system.

alternating the number of lamps that were turned on. In the case with one or two lamps on, the width of lamp plane decreased. In the experiments, the disc/cylinder was always kept under the centre of the lamp plane.

Reagent grade 4-chlorophenol (4-CP) was chosen as the model reactant. The concentration of 4-CP was determined by measuring UV absorbance at 224 nm using an UV–vis wavelength spectrometer (Hewlett Packard, HP8453). Although the UV absorbance at 224 nm includes the absorbance of both 4-CP and those decomposition products which absorb at 224 nm, it provides a measurement of the overall degradation rate of the UV absorbing species. For kinetic analysis, these "UV absorbing species" can be regarded as a kind of model reactant, simply called A_{224}.

Total organic carbon (TOC) was measured by a combustion-type TOC analyzer with an infrared detector (Shimadzu, TOC-500). Incident irradiance from the lamps was measured by a digital radiometer (DRC-100X, Spectroline) with a UV-A sensor (DIX-365, Spectroline). The water film thicknesses on the surface of the drum and disc were measured by weighing the water tank before and after the water film was formed, or by absorbing all the water film using tissue paper, and determining the change in weight. To determine the accuracy of this measurement, a small piece of aluminum plate (ϕ 48 mm), which was coated with P25 TiO_2, was set into water and then taken out to form a water film on the surface. The water film was first measured using the tissue paper absorption method, and then the plate was dried at 105 °C for 2 h. The weight difference before and after drying at 105 °C divided by the total amount of water film, i.e., the relative error due to insufficient absorption, was 6.48%. In this test, the determined thickness of the water film was 29.8 μm.

2.2. Results

To validate the non-volatile characteristics and UV-stability of 4-CP, two blank experiments, photocatalyst without UV and UV without photocatalyst, were conducted. The results showed that the A_{224} concentration did not vary significantly with time.

There are three basic geometric and operating parameters for the rotating disc reactor: rotation speed, angle of teeth, and radiation intensity. A series of experiments were designed and conducted to test these three factors. Figs. 2 through 7 are the results of these experiments, where the initial 4-CP concentrations were 30 mg/dm^3. Fig. 2 indicates that the disc reactor had a higher A_{224} degradation rate, presumably due to a larger illuminated surface and capture of reflected photons. Fig. 3 shows a comparison of the disc and drum reactor performance. In this disc experiment, half of the discs were covered by a UV opaque plate, leaving only half of the discs exposed to UV. Thus the total photon flow rate from the lamp onto the rotating disc reactor was about half of that on the rotating drum. However, due to the 60° angle between discs, the two experimental systems have a similar actual illuminated surface area, and it is noted that the measured degradation rates were also similar. A quantitative discussion will be conducted in following section.

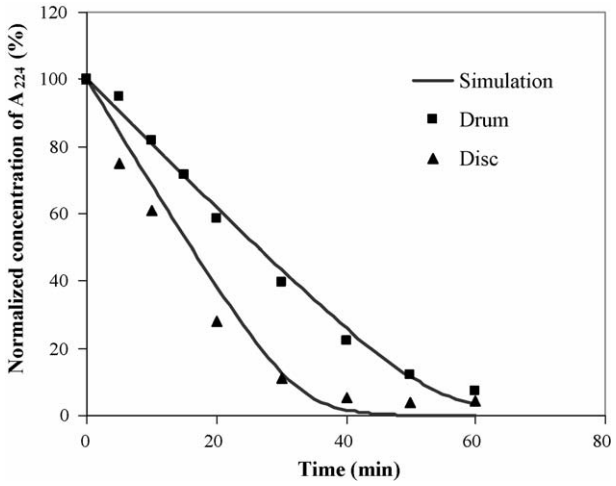

Fig. 2. Time course of 4-CP degradation, with three lamps on, at 20 rpm.

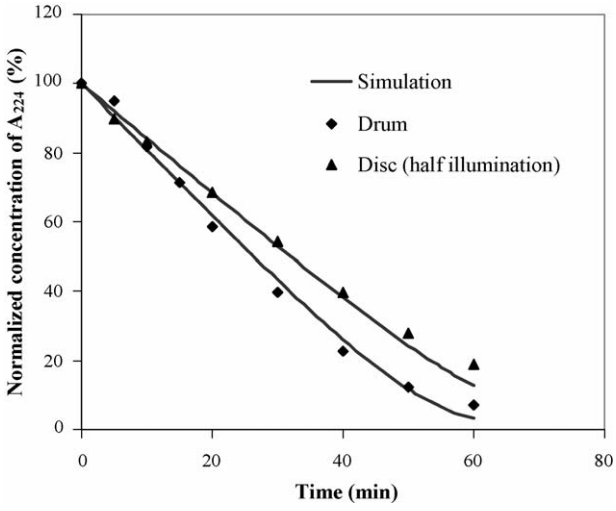

Fig. 3. Time course of 4-CP degradation, with three lamps on, at 20 rpm, but only one half of discs were exposed to the UV lamp (the other half were covered by an opaque plate).

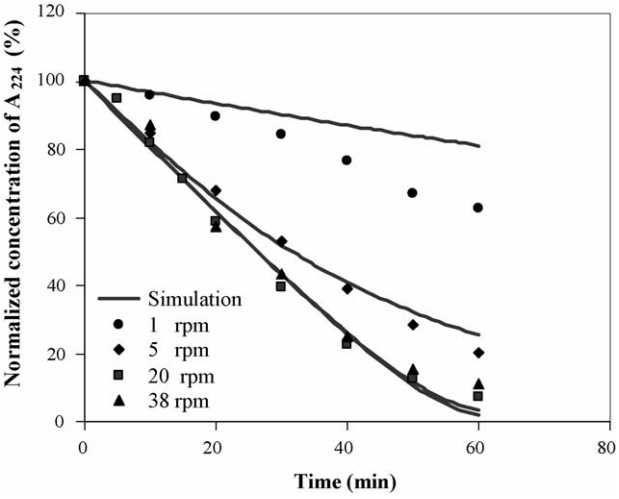

Fig. 4. Time course of 4-CP degradation in rotating drum reactor, with three lamps on.

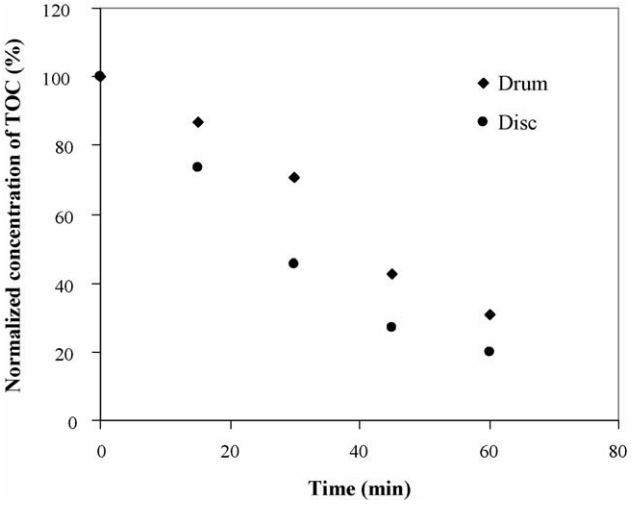

Fig. 5. TOC variations with time, with three lamps on, at 20 rpm.

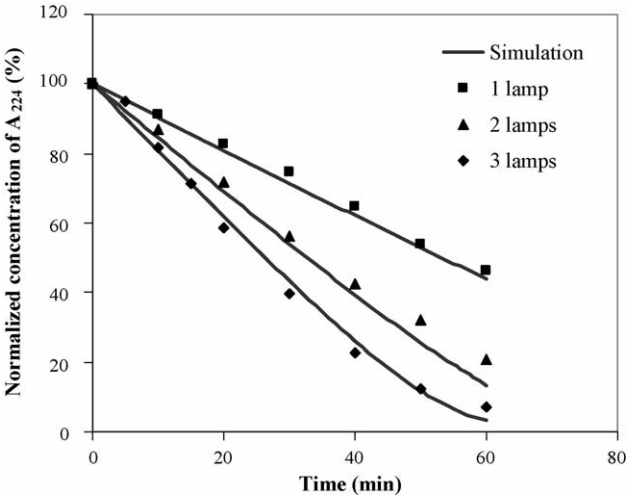

Fig. 6. Time course of 4-CP degradation in rotating drum reactor at 20 rpm.

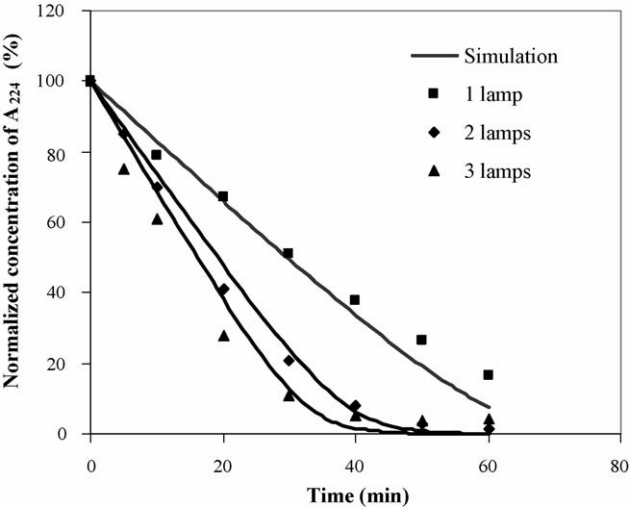

Fig. 7. Time course of 4-CP degradation in rotating disc reactor at 20 rpm.

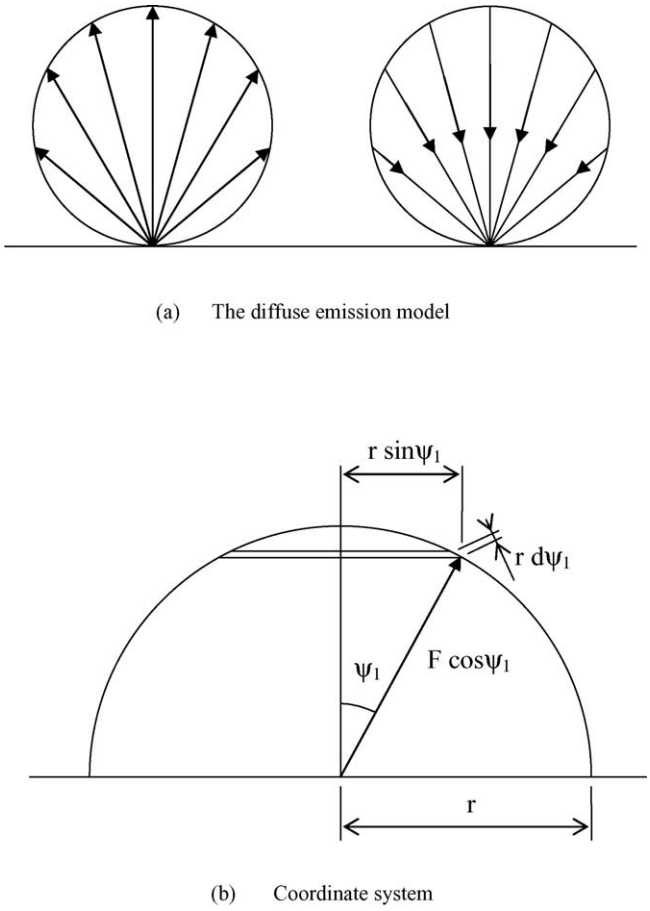

Fig. 8. The diffuse emission model (a) and the coordinate system (b) for calculation.

In literature [9], the influence of the rotation speed is mathematically discussed. When the rotation speed is smaller than a specific value (in this study, this value is between 5 and 20 rpm, see Fig. 4), the water film is too thin to provide organic compound to the photocatalytic surface at a rate which is equal to or larger than the degradation potential of the photocatalyst. In Fig. 4, when the rotation speed was 1 and 5 rpm, this phenomenon can be observed, which indicates that to maintain a sufficient water film thickness is crucial for maximizing the effectiveness of the disc reactor. The TOC variations in Fig. 5 indicate that the 4-CP was not only decomposed, but also was substantially mineralized. Figs. 6 and 7 show the influence of illumination intensity on the degradation process.

3. Discussion

3.1. Analysis of radiation field

3.1.1. Diffuse emission model

The diffuse emission model has been reported to be suitable for modeling fluorescent lamps [11]. For the UV lamp, first we assume that the photons fall on the sleeve in a diffuse way (Fig. 8(a), the incident irradiance on the illuminated plane is proportional to the cosine of the angle of incidence).

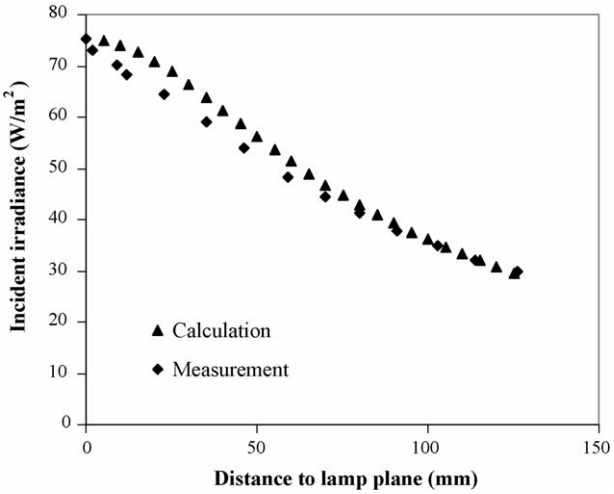

Fig. 9. Radiation field measurements and simulation on the line which is normal to the lamp plane and passes the centre of the plane.

The total radiation power from one point on the UV lamp (Fig. 8(b), the area of the point on the lamp plane is dS) is WdS. According to energy conservation, the energy across the hemi-sphere around this point should be equal to WdS. Mathematically the hemi-sphere is composed of many rings from $\psi_1 = 0^\circ$ to 90° (Fig. 8(b)). The width of rings is $rd\psi_1$ the circumference is $2\pi(r\sin\psi_1)$. Subsequently the area of the rings is $(2\pi(r\sin\psi_1))(rd\psi_1)$. The irradiance in the direction of ψ_1 is $F\cos\psi_1$ (diffuse emission model, see also Fig. 8(a)). Therefore,

$$W\,\mathrm{d}S = \int_0^{\pi/2} F\cos\psi_1(2\pi(r\sin\psi_1))(r\,\mathrm{d}\psi_1) = \pi F r^2 \tag{1}$$

Under the lamp, at an illuminated point, the irradiance from one point of the lamp is $F\cos\psi_1$ (diffuse emission model, see also left figure in Fig. 8(a)), the incident irradiance onto the illuminated point (diffuse emission model, see also right figure in Fig. 8(a)) is

$$w_\mathrm{p} = (F\cos\psi_1)\cos\psi_2 = \frac{W\cos\psi_1\cos\psi_2}{\pi r^2}\,\mathrm{d}S \tag{2}$$

The total incident irradiance from the whole lamp plane on this illuminated point is

$$w = \frac{W}{\pi}\iint_{\text{lamp}} \frac{\cos\psi_1\cos\psi_2}{r^2}\,\mathrm{d}S \tag{3}$$

Fig. 9 shows the radiometer measurement result and simulation by Eq. (3), which closely match each other. Thus the diffuse assumption is shown to be appropriate, and the diffuse emission model is suitable for modeling in this system.

3.1.2. The radiation model for rotating disc reactor

In a photocatalytic reaction, one photon can potentially excite one electron only if the photon energy is larger than the band gap, consequently "einstein" is a more suitable measurement unit than an overall energy unit such as the Joule. Since the

spectral specific irradiance from the UV lamp follows a normal distribution ($\sigma = 15.75$ nm, λavg = 353 nm) [10], the unit change could be

$$W\,(\text{einstein/s/m}^2) = \int_0^{387} \frac{1}{N_A hc/\lambda} \frac{W(\text{J/s/m}^2)}{\sigma\sqrt{2\pi}} e^{-(\lambda-\lambda_{avg})^2/(2\sigma^2)} d\lambda \quad (4)$$

The photon which can excite an electron to jump from the valence band to the conduction band must have energy larger than the band gap of TiO_2 (anatase), 3.2 eV. That is, the wavelength of the photon, which can induce a photocatalytic reaction, must be shorter than 387 nm (=Planck's constant × light velocity/band gap), which is the reason that the upper limit of integration is 387 nm.

Based on Eq. (3), the radiation model, Eq. (4), can be derived using a similar detailed derivation of the radiation model reported elsewhere [10].

The coordinate system was established as shown in Fig. 1(b). The incident irradiance on any point, due to radiation from the lamp, is expressed as

$$I(x', y', z') = \frac{1}{\pi} \iint_{\text{lamp}} \frac{w_\lambda \cos\psi_1 \cos\psi_2}{d_1^2} dx\, dz \quad (5)$$

The incident irradiance on the upper wing due to the reflection from the lower wing is

$$I^{(n)}_{\lambda-uw}(\theta', z') = \frac{1-a(\lambda)}{\pi} \iint_{lw} \frac{I^{(n-1)}_{\lambda-uw}(\theta, -z)\cos\psi_3 \cos\psi_4}{d_2^2} \frac{r_b}{\sin\alpha} d\theta\, dz \quad (6)$$

The local-area-specific rate of energy absorption (LASREA) is

$$q_{uw}(\theta', z') = q_{lw}(\theta', -z') = \int_0^{387} [q^{(0)}_{\lambda-uw}(\theta', z') + q^{(1)}_{\lambda-uw}(\theta', z') + \cdots + q^{(n)}_{\lambda-uw}(\theta', z')]\, d\lambda \quad (7)$$

3.1.3. Simulation results and discussion

Fig. 10 shows the simulated radiation field on the surface of the drum, while Fig. 11 shows the field at values of $z/B = 0.1$, 0.5 and 0.9 on the surface of the disc. In Fig. 10, we can find that the narrow lamp plane, or a fewer number of lamps, shows a narrow shape of distribution. This indicates that a wide lamp plane or a wide layout of lamps is beneficial for providing a relatively uniform radiation field. Fig. 11 shows the distribution of incidence, absorption (with no photon recapture) and LASREA on different cross-sectional surfaces of a disc. Near the valley bottom between discs, a larger difference between LASREA and absorption/no recapture is shown than near the top of a disc tooth. This indicates that the recapture of reflected photons tends to occur most effectively near the valley bottom. Therefore, a deeper valley is beneficial for the capture of reflection, as indicated in previous work on corrugated plates [10].

Table 1 shows the total photon flow rate onto the disc and drum, respectively, when different numbers of lamps are on.

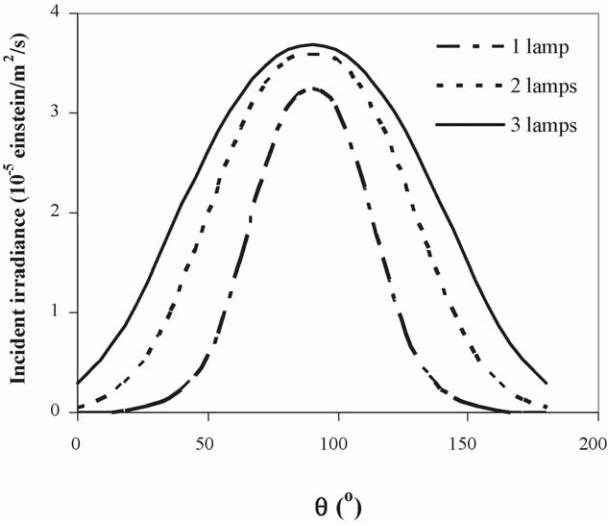

Fig. 10. Irradiance distribution on the surface of rotating disc, $z/B = 0.5$.

Though the disc increases the illumination area, the total photon flow rate is similar to that of drum. Due to the capture of reflected photons, the actual absorbed photon number, LASREA, is increased 11.2% over direct absorption of incident photons from the lamps alone.

3.2. Kinetic analysis

3.2.1. Model

In our previous work, a kinetic relationship for local degradation was established [12]. In this rotating disc reactor, the water film has to be considered, and the model is shown in Table 2. In photocatalytic decomposition of organic compounds, the oxygen plays an important role in the capture of excited electrons:

$$TiO_2 + h\gamma \rightarrow h^+ + e^- \quad (11)$$

$$H_2O \rightarrow OH^- + H^+ \quad (12)$$

$$h^+ + OH^- \rightarrow {}^\bullet OH \quad (13)$$

$$e^- + O_2 \rightarrow O_2{}^- \quad (14)$$

$$O_2{}^- + H^+ \rightarrow {}^\bullet OOH \quad (15)$$

Table 1
Photon flow rate onto the reactor under three UV lamps[a], 10^{-7} einstein/s

		Incidence	Absorption/no recapture	LASREA
One lamp	Drum	4.105	2.270	–
	Disc	4.21	2.33	2.58
Two lamps	Drum	7.307	4.040	–
	Disc	7.29	4.03	4.53
Three lamps	Drum	9.477	5.240	–
	Disc	9.17	5.07	5.64
	Disc (deeper valley)	8.00	4.43	4.85

[a] The incidence was evaluated using Eq. (5); the LASREA was evaluated using Eq. (7), the absorption coefficients were cited from [10].

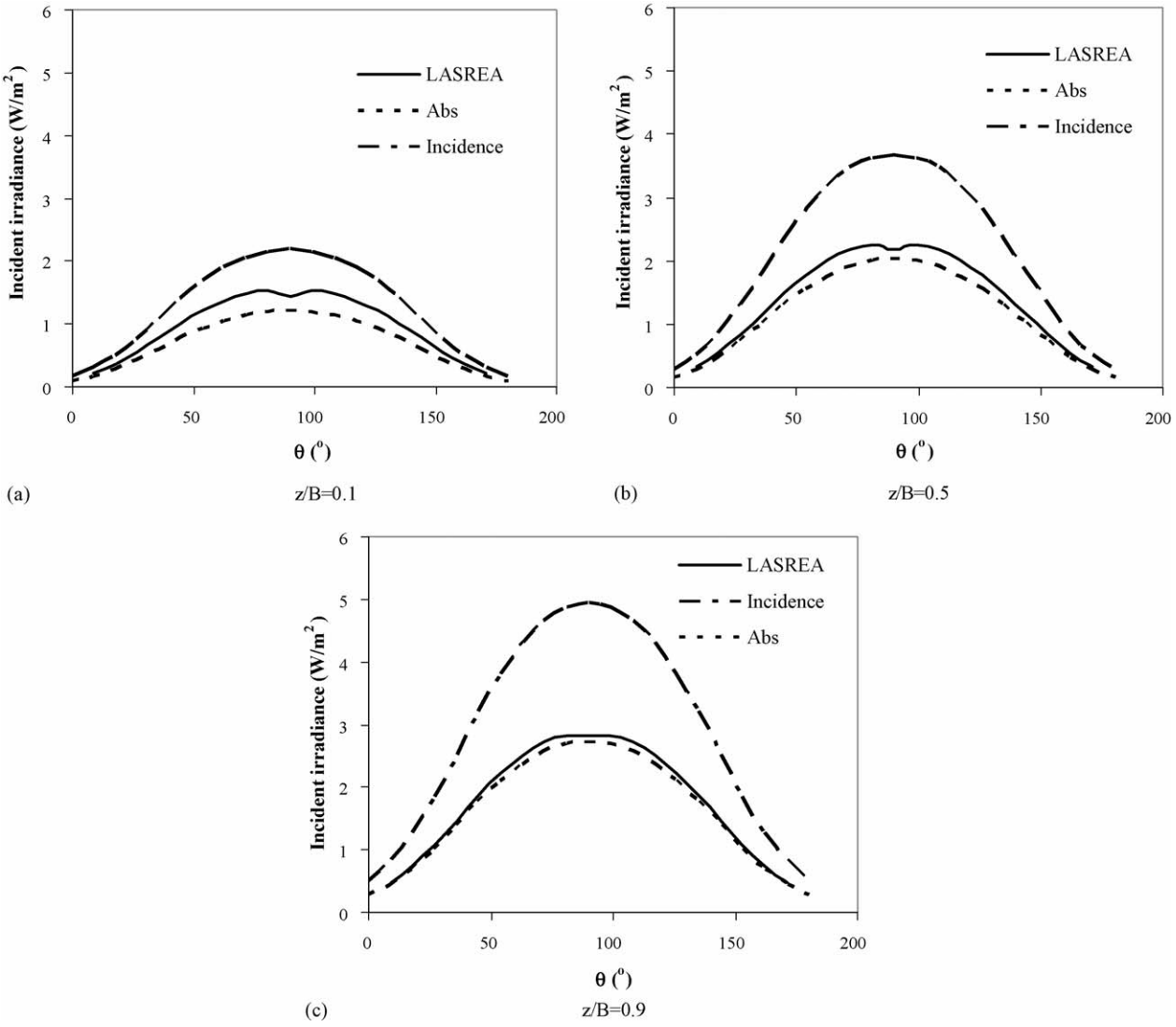

Fig. 11. Distribution of incidence, absorption/no recapture and LASREA on the surface of rotating disc, with three lamps on, at different dimensionless distances from the disc top.

Table 2
Kinetic equations for rotating disc or drum reactor

		Drum	Disc	
In water	Equation	$\frac{\mathrm{Cr}(t)+QC(t)}{V}=\frac{\mathrm{d}C(t)}{\mathrm{d}t}$		(8)
	Boundary condition	$C(0)=C_0$		
On surface	Equation	$\delta=a\omega\phi+b$		(9)
		$\phi=2r_\mathrm{b}$	$\phi=\frac{2z}{\tan\alpha}+2r_\mathrm{s}$	
		$Q=\delta L\omega r$	$Q=\frac{L}{e}\int_0^e\frac{\delta\omega r\,\mathrm{d}z}{\sin\alpha}$	
		$\frac{\delta\,\mathrm{d}C(t,\theta,z)}{\mathrm{d}t}=\frac{kC(t,\theta,z)}{1+KC(t,\theta,z)}\left(\frac{q(\theta,z)}{q_0}\right)^n$		(10)
		$\mathrm{Cr}(t)=QC(t,\theta_\mathrm{end},z)$	$Cr(t)=\int_0^e\frac{C(t,\theta_\mathrm{end},z)\delta\omega r\,\mathrm{d}z}{\sin\alpha}$	
	Boundary condition	$C(t,0,z)=C(t)$		

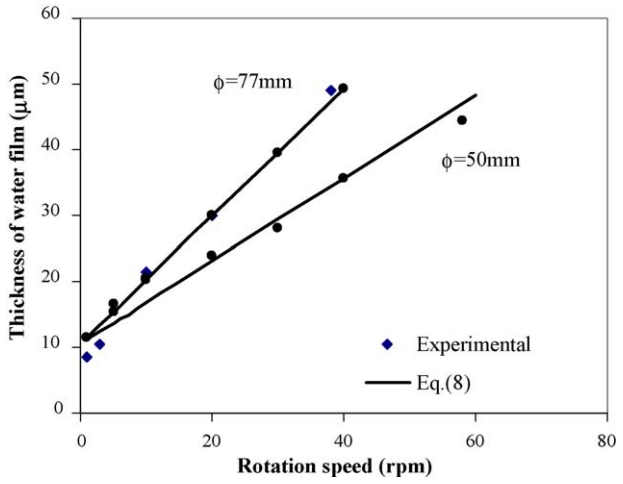

Fig. 12. Thickness of water film vs. rotation speed.

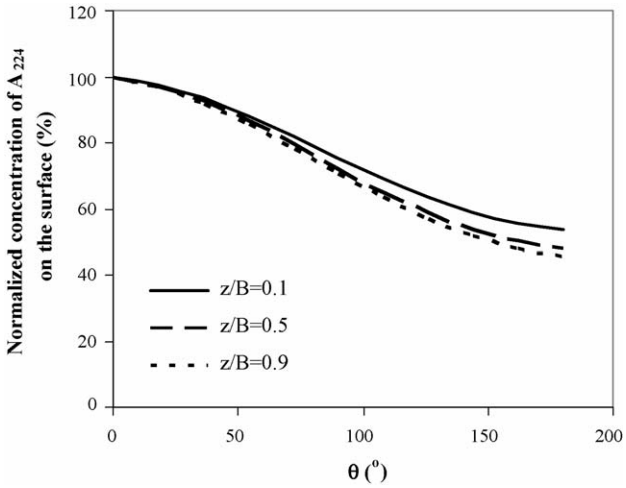

Fig. 13. Typical concentration profile on the surface of disc at 20 rpm, three lamps on, at $t = 30$ min.

$$^{\bullet}\mathrm{OH\ and/or\ }^{\bullet}\mathrm{OOH} + \text{organic compounds} \rightarrow \cdots \rightarrow \mathrm{H_2O} + \mathrm{CO_2} \quad (16)$$

In this rotating disc reactor, the oxygen is continuously provided from the atmosphere, that is, the oxygen in atmosphere must penetrate the water film to reach the surface of photocatalyst. The flux N_{O_2} of oxygen diffusing in the water film observes Fick's first law:

$$N_{O_2} = -D\frac{dC_{O_2}}{dR} \quad (17)$$

Considering the extreme situation where oxygen is saturated at the water surface adjacent to the air, 2.501×10^{-5} (mole fraction, 20° C) [13], and completely consumed at the surface of photocatalyst, i.e., the concentration is 0, we can estimate the diffusion flux from Eq. (17) as $N_{O_2} > 1.49 \times 10^{-4}$ mg/cm^2 s when the thickness of water film is less than 60 μm (in this study, the maximum is less than 60 μm, see Fig. 12). On the other hand, the amount of oxygen which is stoichiometrically necessary to mineralize 160 ml of 30 ppm 4-CP in 60 min (the concentration and the time we used in the experiment) is 1.288×10^{-5} mg/cm^2 s, which is much smaller than N_{O_2} ($1.49 \times 10^{-4} >$ mg/cm^2 s). Consequently, oxygen supply does not appear to be a rate-limiting step for this photocatalytic reaction, and it is not necessary to insert an oxygen factor into the kinetics (Eq. (10) in Table 2). In this reactor, the thickness of the water film is a crucial factor, and its value is very small, <60 μm. The mass transfer on the surface of the disc/drum can be expressed as a mass flux onto the surface (Eq. (8) in Table 2). In the model equation, Eq. (10), q_0 is the reference value of the local-area-specific rate of energy absorption. For model fitting purposes, this value could be chosen arbitrarily within a rational range, and then correspondingly the parameter k could be adjusted so as to maintain a constant $kq_0{}^{-n}$. Here q_0 is designated as 10^{-5} einstein m^{-2}s^{-1}.

Due to the low conversion per rotation and the small water tank volume, the system is similar to a completely mixed reactor; which was verified by comparing experiments with and without stirring in the water tank. Eq. (8) in Table 2 shows the mass balance in the reaction system, composed of the rotating disc and water tank.

The parameters in the model are cited from our previous work [12]. The value of k was adjusted/fitted partially because a different unit of irradiance is used, resulting in $k = 1.10 \pm 0.05$ m/h, $K = 0.573 \pm 0.012$ m^3/g, and $n = 0.52 \pm 0.032$.

The thickness of water film is determined by Eq. (9) in Table 2. This equation is a statistical fitting result, which appears a linear relation between the thickness of water film and the velocity of the drum surface, given as the radius times rotation speed. Fig. 12 shows the measurement results of the mean thickness of water film on the surface of rotating drums of $\phi = 50$ mm [9] and 77 mm, respectively, and calculated results using Eq. (9). The successful fitting between them indicates that the equation is a good expression of the mathematical relationship between water film thickness, rotation speed and diameter of the disc or drum in the range 50 mm $< \phi <$ 77 mm. In the following kinetic simulation, the diameter to estimate thickness of water film is in the range 54.6 mm $\leq \phi \leq$ 77 mm, which lies between 50 and 77 mm. Therefore, the estimation is in good accuracy, and in Fig. 12, $a = 1.26 \times 10^{-5}$ min, $b = 10.5$ μm.

3.2.2. Simulation results and discussions

The radiation field analysis provided the LASREA distribution, which is the basis of the photocatalytic kinetics. We can apply Eqs. (8)–(10) to calculate the concentration distribution on the surface of the reactor in accordance with the LASREA distribution. Fig. 13 shows three concentration profiles of 4-CP on the surface of the disc at $z/B = 0.1$, 0.5, and 0.9, respectively. The profile shows a "reverse S" shape. The inflection point from convex to concave is at $\theta = 90°$, which is identical to the radiation distribution, where the irradiance reaches a maximum at $\theta = 90°$. On the valley bottom between discs (small z/B), the profile shows a higher concentration than on the top of disc tooth (large z/B), which is the response to the radiation distribution shown in Figs. 10 and 11. The simulation results corresponding to each experimental condition have been shown in Figs. 2 through 7,

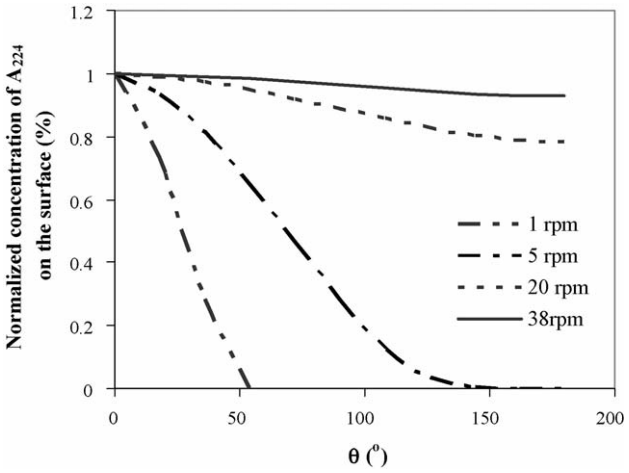

Fig. 14. The predicted 4-CP distribution profile on the surface of the drum at $t = 30$ min, with three lamps on.

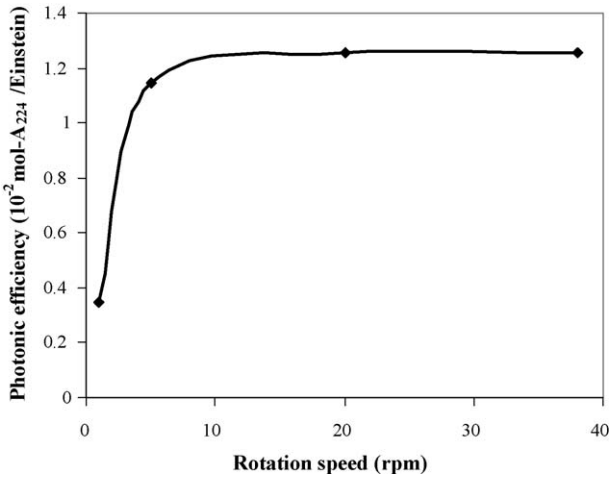

Fig. 15. The photonic efficiency vs. rotation speed of disc at $t = 20$ min when three lamps are on.

where it is noted that the agreement between experiment and simulation is very good. Fig. 14 is the concentration distribution on the surface of a drum corresponding to Fig. 4. When the thickness of the water film is very small and it remains on the illuminated surface for too long a time, the organic concentration becomes zero before the water film returns to the water tank. That is, in such a case the "bottleneck" of the degradation process is mass transfer of the organic. That indicates that at low rotation speed, part of the photocatalyst area is wasted since mass transfer is too slow to match the reaction speed.

According to radiation and kinetic analysis, we can further observe the apparent photonic efficiency, defined as follows:

$$\Phi = \frac{(C(t) - C(0))V}{t\varphi M_{4\text{-CP}}} \tag{18}$$

Since $C(t)$ is not linear with time, the photonic efficiency will change with time as well. However, in Figs. 2–7 (except for Fig. 5), the linear regression correlation coefficient (R^2) of the experimental data within 20 min is between 0.9506 and 0.9999 (in fact, eight out of 10 curves have R^2 greater than 0.9851) that is, in the initial stage within 20 min, the concentration varies approximately linearly with time. So we used the data at the 20th minute to analyze photonic efficiency. Fig. 15 shows the relationship between rotation speed and photonic efficiency. It is evident that rotation speed is an important factor in the photonic efficiency. The higher the rotation speed is, the higher the photonic efficiency. As can be seen in Fig. 16, low radiation (one lamp) has a higher photonic efficiency, which agrees with other reported research [8]. Fig. 16 also indicates that the disc reactor has an approximately 70% higher photonic efficiency than the drum reactor. In the drum reactor, the maximum photonic efficiency (Φ) of degradation is 0.0145 mol-4-CP/einstein, while in the disc reactor, 0.0251 mol-4-CP/einstein (20 rpm, one lamp). For mineralization, Φ is 0.0143 mol C/einstein in the drum reactor, and 0.0266 mol C/einstein in the disc reactor (20 rpm, three lamps). The radiation field analysis has indicated that the disc has a similar incident photon flow rate, and the capture of reflected photon can result in an 11.2% increase, but the photonic efficiency of the disc reactor is nearly two times of that of drum reactor. This indicates that the reason for the higher efficiency of the disc is mainly due to the increase of illuminated area. In the disc reactor, with a 60° angle between discs, the illuminated area is about twice that of the drum. Such a result shows an important fact that when the light source is fixed, to distribute limited photons onto more photocatalyst area is an effective principle for engineering design.

3.3. Crucial factors for scale-up

The radiation distribution for a rotating disc reactor with a deeper valley (two times that used in experiments) and the same disc angle, 60°, was simulated. The LASREA is 9.48% greater than absorption/no recapture. Compared with a shallow valley (11.2%), the recaptured photon number decreased due to a decrease in the number of discs. The illumination area is constant since the same angle between teeth is used. On the other hand, a deep valley introduces a bigger average distance between the light source and the photocatalyst, resulting in an increase of photon loss. The prediction of removal ratio of 4-CP in 20 min is 53.60% (20 rpm), which is less than the shallow valley situation

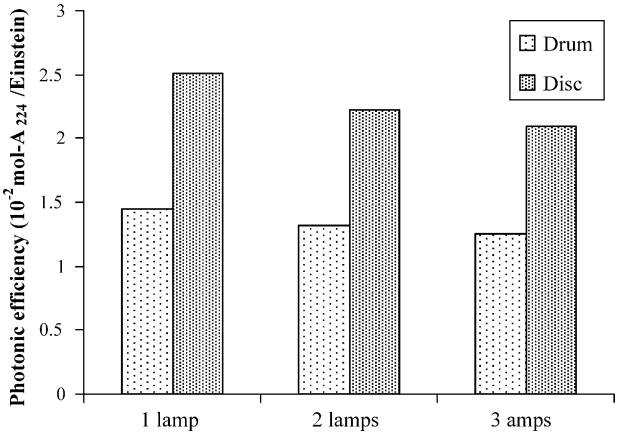

Fig. 16. Photonic efficiency vs. lamp number, at 20 rpm, $t = 20$ min.

with 61.62%. Therefore, a shallow valley and small angle are recommended in engineering design.

When the light source is geometrically narrow, the illuminated area decreases and radiation distribution is more non-uniform (Fig. 10). In a laboratory scale, it is easy to keep a lamp width larger than the disc diameter, however when scaled-up, rational layout of the lamps will be important.

The rotation speed is related to the thickness of the water film, which has a significant influence on the degradation process. Although many factors, such as viscosity and temperature, influence the formation and thickness of the water film, if just scaling up the reactor these physical factors would be constant. Subsequently in mechanical design, the determining factor for the water film thickness is rotation speed and diameter of the disc/drum. When the disc diameter is scaled up, the rotation speed has to be increased to maintain a sufficient thickness of water film on the surface.

4. Conclusions

In this work, the proposed rotating disc reactor was analyzed kinetically, based on experiments and simulation of the radiation field. The model suggested in this paper includes the thickness of water film and irradiance, which are the most important factors for such a reactor. The experimental results and mathematical simulations reveal:

(1) The configuration using discs has larger illuminated area, but the photon flow rate onto the disc is similar to that of the drum.
(2) The thickness of the water film on the surface of disc/drum is a crucial factor for this rotating reactor, and it is determined by both rotation speed and disc diameter. A semi-empirical equation to estimate thickness of the water film was established.
(3) Though deeper valleys in the disc reactor can increase the capture of reflected photons, it has little influence on the photonic efficiency compared with the influence of the illumination area. A shallow valley and small angle are recommended.
(4) Low radiation intensity produces a higher photonic efficiency. The radiation distribution is sensitive to the layout of lamps. Keeping a uniform distribution is an important principle in engineering design.
(5) The mathematical model introduced in this paper is an effective tool to simulate the experiments and provide design data.

Acknowledgements

Special thanks are given to Prof. Tatso Kanki at the Department of Chemical Engineering, Himeji Institute of Technology, Japan, and Dr. Atsushi Toyoda, the Managing Director of Envysis Co. Ltd., Japan, who supervised Ph.D. work by L. Zhang related to this research. This work was supported by the Natural Sciences and Engineering Research Council of Canada.

References

[1] A. Fujishima, K. Honda, Electrochemical photolysis of water at a semiconductor electrode, Nature 238 (1972) 37–38.
[2] M.R. Hoffmann, S.T. Martin, W. Choi, D.W. Bahnemann, Environmental applications of semiconductor photocatalysis, Chem. Rev. 95 (1995) 69–96.
[3] D.D. Dionysiou, M.T. Suidan, I. Baudin, J.-M. Laine, Oxidation of organic contaminants in a rotating disk photocatalytic reactor: reaction kinetics in the liquid phase and the role of mass transfer based on the dimensionless Damkohler number, Appl. Catal. B: Environ. 38 (2002) 1–16.
[4] P.F.R. Nogueira, W.F. Jardim, TiO_2-fixed-bed reactor for water decontamination using solar light, Sol. Energy 56 (1996) 471–475.
[5] M. Bekbölet, M. Lindner, D. Weichgrebe, K.W. Bahnemann, Photocatalytic detoxification with the thin-film fixed-bed reactor (TFFBR): clean-up of highly polluted landfill effluents using a novel TiO_2-photocatalyst, Sol. Energy 56 (1996) 455–469.
[6] P. Wyness, J.F. Klausner, D.Y. Goswami, K.S. Schanze, Performance of noncentrating solar photocatalytic oxidation reactors. Part I. Flat-plate configuration, J. Sol. Energy Eng. 116 (1994) 2–7.
[7] N.Z. Muradov, Solar detoxification of nitroglycerine-contaminated water using immobilized titania, Sol. Energy 52 (1994) 283–288.
[8] Y. Ohko, K. Hashimoto, A. Fujishima, Kinetics of photocatalytic reactions under extremely low-intensity UV illumination on titanium dioxide thin films, J. Phys. Chem. A 101 (1997) 8057–8062.
[9] L. Zhang, T. Kanki, N. Sano, A. Toyoda, Photocatalytic degradation of organic compounds in aqueous solution by a TiO_2 photocatalyst coated rotating-drum reactor using solar light, Sol. Energy 70 (2001) 331–337.
[10] Z. Zhang, W.A. Anderson, M. Moo-Young, Rigorous modeling of UV absorption by TiO_2 films in a photocatalytic reactor, AIChE J. 46 (2000) 1461–1470.
[11] O.M. Alfano, R.L. Romero, A.E. Cassano, Radiation field modeling in photoreactors — 1 homogeneous media; 2 heterogeneous media, Chem. Eng. Sci. 41 (1986) 421–444.
[12] Z. Zhang, W.A. Anderson, M. Moo-Young, Modeling of corrugated plate photocatalytic reactors and experimental validation, Chem. Eng. Sci. 58 (2003) 911–914.
[13] D.R. Lide, CRC Handbook of Chemistry and Physics, 85th ed., CRC Press, Boca Raton, 2004–2005, pp. 8–88.